Research Article | Vol. 25, No. 5 | 6 Mar 2017 | OPTICS EXPRESS 4655

Optics EXPRESS

Resonance optical trapping of individual dye-doped polystyrene particles with blue- and red-detuned lasers

TETSUHIRO KUDO,[1,3] HAJIME ISHIHARA,[2] AND HIROSHI MASUHARA[1,4]

[1]*Department of Applied Chemistry, College of Science, National Chiao Tung University, Hsinchu 30010, Taiwan*
[2]*Department of Physics and Electronics, Osaka Prefecture University, Sakai, Osaka 599-8531, Japan*
[3]*kudo@nctu.edu.tw*
[4]*masuhara@masuhara.jp*

Abstract: We demonstrate resonance optical trapping of individual dye-doped polystyrene particles with blue- and red-detuned lasers whose energy are higher and lower compared to electronic transition of the dye molecules, respectively. Through the measurement on how long individual particles are trapped at the focus, we here show that immobilization time of dye-doped particles becomes longer than that of bare ones. We directly confirm that the immobilization time of dye-doped particles trapped by the blue-detuned laser becomes longer than that by the red-detuned one. These findings are well interpreted by our previous theoretical proposal based on nonlinear optical response under intense laser field. It is discussed that the present result is an important step toward efficient and selective manipulation of molecules, quantum dots, nanoparticles, and various nanomaterials based on their quantum mechanical properties.

OCIS codes: (140.7010) Laser trapping; (260.5740) Resonance; (350.4855) Optical tweezers or optical manipulation.

References and links

1. A. Ashkin, J. M. Dziedzic, J. E. Bjorkholm, and S. Chu, "Observation of a single-beam gradient force optical trap for dielectric particles," Opt. Lett. **11**(5), 288–290 (1986).
2. M. Righini, A. S. Zelenina, C. Girard, and R. Quidant, "Parallel and selective trapping in a patterned plasmonic landscape," Nat. Phys. **3**(7), 477–480 (2007).
3. N. A. Grigorenko, W. N. Roberts, R. M. Dickinson, and Y. Zhang, "Nanometric optical tweezers based on nanostructured substrates," Nat. Photonics **2**(6), 365–370 (2008).
4. T. Shoji, Y. Mizumoto, H. Ishihara, N. Kitamura, M. Takase, K. Murakoshi, and Y. Tsuboi, "Plasmon-based optical trapping of polymer nano-spheres as explored by confocal fluorescence microspectroscopy: a possible mechanism of a resonant excitation effect," Jpn. J. Appl. Phys. **51**(9R), 092001 (2012).
5. Y. Pang, and R. Gordon, "Optical trapping of a single protein," Nano Lett. **12**(1), 402–406 (2012).
6. T. Shoji, and Y. Tsuboi, "Plasmonic optical tweezers toward molecular manipulation: tailoring plasmonic nanostructure, light source, and resonant trapping," J. Phys. Chem. Lett. **5**(17), 2957–2967 (2014).
7. B. Agate, C. Brown, W. Sibbett, and K. Dholakia, "Femtosecond optical tweezers for in-situ control of two-photon fluorescence," Opt. Express **12**(13), 3011–3017 (2004).
8. L. Pan, A. Ishikawa, and N. Tamai, "Detection of optical trapping of CdTe quantum dots by two-photon-induced luminescence," Phys. Rev. B **75**(16), 161305 (2007).
9. A. K. De, D. Roy, A. Dutta, and D. Goswami, "Stable optical trapping of latex nanoparticles with ultrashort pulsed illumination," Appl. Opt. **48**(31), G33–G37 (2009).
10. Y. Jiang, T. Narushima, and H. Okamoto, "Nonlinear optical effects in trapping nanoparticles with femtosecond pulses," Nat. Phys. **6**(12), 1005–1009 (2010).
11. A. Usman, W. Y. Chiang, and H. Masuhara, "Optical trapping and polarization-controlled scattering of dielectric spherical nanoparticles by femtosecond laser pulses," J. Photochem. Photobiol. Chem. **234**, 83–90 (2012).
12. A. Kittiravechote, W. Y. Chiang, A. Usman, I. Liau, and H. Masuhara, "Enhanced optical confinement of dye-doped dielectric nanoparticles using a picosecond-pulsed near-infrared laser," Laser Phys. Lett. **11**(7), 076001 (2014).
13. T. H. Liu, W. Y. Chiang, A. Usman, and H. Masuhara, "Optical trapping dynamics of a single polystyrene sphere: continuous wave versus femtosecond lasers," J. Phys. Chem. C **120**(4), 2392–2399 (2016).
14. M. A. Osborne, S. Balasubramanian, W. S. Furey, and D. Klenerman, "Optically biased diffusion of single molecules studied by confocal fluorescence microscopy," J. Phys. Chem. B **102**(17), 3160–3167 (1998).

#283211 https://doi.org/10.1364/OE.25.004655
Journal © 2017 Received 4 Jan 2017; revised 12 Feb 2017; accepted 14 Feb 2017; published 21 Feb 2017

Optics EXPRESS

15. G. Chirico, C. Fumagalli, and G. Baldini, "Trapped Brownian motion in single- and two-photon excitation fluorescence correlation experiments," J. Phys. Chem. B **106**(10), 2508–2519 (2002).
16. H. Li, D. Zhou, H. Browne, and D. Klenerman, "Evidence for resonance optical trapping of individual fluorophore-labeled antibodies using single molecule fluorescence spectroscopy," J. Am. Chem. Soc. **128**(17), 5711–5717 (2006).
17. C. Hosokawa, H. Yoshikawa, and H. Masuhara, "Enhancement of biased diffusion of dye-doped nanoparticles by simultaneous irradiation with resonance and nonresonance laser beams," Jpn. J. Appl. Phys. **45**(16), L453–L456 (2006).
18. M. Dienerowitz, M. Mazilu, P. J. Reece, T. F. Krauss, and K. Dholakia, "Optical vortex trap for resonant confinement of metal nanoparticles," Opt. Express **16**(7), 4991–4999 (2008).
19. M. J. Kendrick, D. H. McIntyre, and O. Ostroverkhova, "Wavelength dependence of optical tweezer trapping forces on dye-doped polystyrene microspheres," J. Opt. Soc. Am. B **26**(11), 2189–2198 (2009).
20. T. Shoji, N. Kitamura, and Y. Tsuboi, "Resonant Excitation effect on optical trapping of Myoglobin: The important role of a Heme cofactor," J. Phys. Chem. C **117**(20), 10691–10697 (2013).
21. M. L. Juan, C. Bradac, B. Besga, M. Johnsson, G. Brennen, G. Molina-Terriza, and T. Volz, "Cooperatively enhanced dipole forces from artificial atoms in trapped nanodiamonds," Nat. Phys. (to be published).
22. R. Agayan, F. Gittes, R. Kopelman, and C. F. Schmidt, "Optical trapping near resonance absorption," Appl. Opt. **41**(12), 2318–2327 (2002).
23. T. Iida, and H. Ishihara, "Theoretical study of the optical manipulation of semiconductor nanoparticles under an excitonic resonance condition," Phys. Rev. Lett. **90**(5), 057403 (2003).
24. T. Iida, and H. Ishihara, "Theory of resonant radiation force exerted on nanostructures by optical excitation of their quantum states: From microscopic to macroscopic descriptions," Phys. Rev. B **77**(24), 245319 (2008).
25. C. S. Adams, and E. Riis, "Laser cooling and trapping of neutral atoms," Prog. Quantum Electron. **21**(1), 1–79 (1997).
26. T. Kudo, and H. Ishihara, "Proposed nonlinear resonance laser technique for manipulating nanoparticles," Phys. Rev. Lett. **109**(8), 087402 (2012).
27. T. Kudo, and H. Ishihara, "Resonance optical manipulation of nano-objects based on nonlinear optical response," Phys. Chem. Chem. Phys. **15**(35), 14595–14610 (2013).
28. L. Novotny, and B. Hecht, *Principles of Nano-Optics* (Cambridge University Press, 2006).
29. T. Kudo, and H. Ishihara, "Two-color laser manipulation of single organic molecules based on nonlinear optical response," Eur. Phys. J. B **86**(3), 98 (2013).

1. Introduction

A laser beam tightly focused into solution can be used to three-dimensionally trap micro- and nano-sized objects at the focus, which is known as optical trapping and optical tweezers [1]. Radiation force is exerted on the objects and it can be classified into scattering force, absorption force and gradient force. The momentum of light is transferred to the objects through the dissipative process such as scattering and absorption, and the objects are pushed toward the direction of laser propagation. The gradient force is induced by electromagnetic interaction between light and induced polarization of the objects. The objects are attracted at the focal spot where the electromagnetic interaction potential is deeper than the surroundings. Recently beyond the conventional optical trapping, locally enhanced light field around plasmonic metal nanostructures [2–6], and pico- and femto-second laser pulses [7–13] are utilized for the optical trapping studies.

The resonance optical trapping using the laser whose energy is resonant to electronic transition of the objects is conceptually important and interesting. The induced polarization can be resonantly enhanced and consequently the resonance radiation force can be increased. There are experimental studies of resonance optical trapping utilizing the continuous wave and pulse lasers [4,5,12,14–21], and theoretical studies based on linear optical response [22–24]. Previously, we have theoretically shown that resonance optical manipulation can be used to selectively sort the semiconductor nanoparticles depending on their electronic transition states [23,24]. This means that molecules, quantum dots, and nanoparticles can be manipulated based on their quantum mechanical properties.

The resonance radiation force depends on the detuning of the laser wavelength. Based on a simple two-level model of objects within linear optical response, the attractive force is exerted on the object with the trapping laser red-detuned from its electronic resonance peak [22] and the blue-detuned laser induces the repulsive force [25]. These are because the electric field and induced polarization are in and out of phase for red- and blue-detuned lasers,

Optics EXPRESS

respectively. In fact, Kendrick et al. experimentally demonstrated that an optical trapping stiffness is enhanced with the red-detuned laser by comparing the trapping of 1 μm dye-doped microparticle and bare one [19]. They also performed the experiment with blue-detuned laser, where the dye-doped microparticle was not stably trapped at the focus. The particle was trapped for a while (~10 s) and diffuse out from the focus. Similarly, efficient trap with red-detuned laser and inefficient trap with blue-detuned one are reported recently through the optical trapping experiment with fluorescent nanodiamonds [21]. Dienerowitz et al. conducted the confinement of gold nanoparticles at the center of vortex beam where the laser intensity is identically zero with utilizing the repulsive force of the blue-detuned laser [18]. These results are explained based on the analysis within linear optical response.

On the other hands, some experimental reports indicate that the blue-detuned laser can be also utilized for efficient optical trapping. There are the experimental reports which observed the biased diffusion of dye molecule and antibody labeled by dye-molecule by using the blue- [14,16,17] and the red-detuned lasers [15,20]. Dye-doped nanoparticles were efficiently trapped by the blue-detuned laser enhanced by plasmonic metal nanostructures [4]. Therefore, these experimental results cannot be explained by linear optical response theory based on two-level model.

Motivated by these experimental facts and in order to understand this contradiction, we have already proposed the nonlinear optical response theory of the radiation force based on three level system dye [26,27]. Under the high laser intensity required for the trapping of dye molecule and nanoparticles, it is necessary to take into account the nonlinear optical effect to our theoretical frameworks. We calculated the radiation force exerted on the dye molecule, and found that the blue-detuned laser give a deeper optical potential than that by the red-detuned laser. We concluded that this is due to the inversion population which matches the phase of the induced polarization to the electric fields even with the blue-detuned laser.

Here, we experimentally demonstrate the resonance optical trapping of individual dye-doped polystyrene particles and bare ones (both are 500 nm in diameter) with blue- and red-detuned lasers, in order to verify our theoretical proposal. Through the measurement on immobilization time of the particles, we found optical trapping with blue-detuned laser provides deeper optical potential compared with that of red-detuned one, which well supports our theoretical proposal.

2. Sample and optical setup

Figure 1(a) shows the optical system where three-dimensional manipulation is demonstrated not only along *z*-axis but also in *xy*-plane for the present polystyrene particles. Emission and excitation spectra of the sample are shown in Fig. 1(b). For the blue- and red-detuned trapping lasers, we used 515 nm (Omicron: LuxX diode laser 515-80, 2.41 eV) and 532 nm (Spectra Physics: Excelsior, 2.33 eV) continuous wave lasers. The beam diameters are about 5 mm adjusted by the collimation lens, and these lasers are tightly focused into the solution with oil immersion objective lens (x100, NA 1.4, Olympus). The focal height from the bottom side of the glass substrate is 50 μm, and the polarization state of the both lasers is linear. The laser power denoted in this work is all measured at the focal plane. Transmission images through a halogen lamp are captured by CCD camera (Watec WAT-232S, 30 frame per second) and notch filters (Semrock: NF03-532E-25 or NF03-514E-25) are used to cut the signal of the trapping lasers from the images.

As a sample, we used dye-doped polystyrene particles (Cat#18720, Polyscience, Inc.) and bare polystyrene particles. (Cat#07307, Polyscience, Inc.) The mean diameter of both particles is 500 nm. The sample solution is diluted by water (the particle concentration is between about 10^7 and 10^8 particles/ml) to avoid the trapping of second particle during individual trapping. After the sonication for 10 min, the sample solution was sandwiched with glass substrates with a spacer (Matsunami) which thickness is about 120 μm. Figure 1(a) indicates excitation and emission spectra of the dye-doped polystyrene particles in water and

Optics EXPRESS

the resonance peak is located at 524 nm in wavelength (2.37 eV in photon energy). The excitation spectrum is detected at 570 nm and the emission spectrum is measured with the excitation at 510 nm. The photon energies of blue- and red-detuned lasers are both shifted by about 40 meV from the resonance peak, and the intensity of excitation spectra at the wavelength of red- and blue-detuned lasers is almost the same. We consider that our experimental condition enables us to directly compare the blue- and red-detuned laser trappings.

For the measurement of the optical trapping behavior, one of simple measurement is to observe the increase in particle numbers at the focal spot. However the optical potential becomes increasingly deeper with increasing the number of particles. Therefore this method is not appropriated to discuss the difference in optical potential. One typical method for evaluating the optical potential is to measure an optical stiffness by analyzing the movement of trapped single particle. The stable trapping is required and the optical potential is modelled as harmonic potential. In the present study, we examine the optical trapping under the relatively shallow optical potential for measuring the immobilization time, where the particle escapes from the focal spot after it is trapped for a while. The analysis method is similar to the paper recently reported [5,13]. We consider that this method allows us to evaluate the optical potential under the balance between optical force and thermally driven random force.

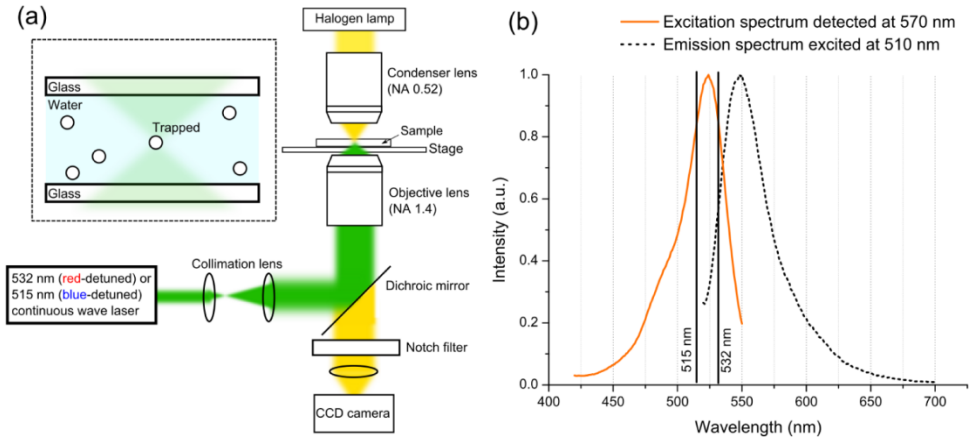

Fig. 1. (a) Setup for optical trapping of individual particles. An inset represents the sample chamber sandwiched by glass substrates and the laser is focused inside the solution. (b) Excitation (solid line) and emission (dashed line) spectra of dye-doped polystyrene particles in water solution. Vertical lines correspond to the wavelength of blue- (515 nm) and red- (532 nm) detuned lasers.

3. Brownian dynamics simulation

In addition, we conducted Brownian dynamics simulation with changing the depth of optical potential and computationally measured the immobilization time to estimate the optical potential. From Langevin equation, the particle position ($\boldsymbol{r}$) and velocity ($\boldsymbol{v}$) for each time step under the optical potential and thermal fluctuation can be expressed as

$$\boldsymbol{r}(t+h)=\boldsymbol{r}(t)+\frac{m}{\xi}\boldsymbol{v}(t)\left\{1-\exp\left(-\frac{\xi}{m}h\right)\right\}+\frac{1}{\xi}\boldsymbol{F}_r(\boldsymbol{r})\left\{h-\frac{m}{\xi}\left(1-\exp\left(-\frac{\xi}{m}h\right)\right)\right\}+\Delta\boldsymbol{r}_B, \tag{1}$$

$$\boldsymbol{v}(t+h)=\boldsymbol{v}(t)\exp\left(-\frac{\xi}{m}h\right)+\frac{1}{\xi}\boldsymbol{F}_r(\boldsymbol{r})\left(1-\exp\left(-\frac{\xi}{m}h\right)\right)+\Delta\boldsymbol{v}_B, \tag{2}$$

Optics EXPRESS

where t, h, m, ξ, $\boldsymbol{F}_r$, $\Delta\boldsymbol{r}_B$ and $\Delta\boldsymbol{v}_B$ are time, interval time, mass of the particle, friction coefficient, radiation force, random displacement of position and velocity, respectively. The mass is calculated from the volume and density (here we assumed the density to be 1.04 g/cm^3). The friction coefficient is $\xi = 3\pi\eta d$, where η and d are solution viscosity (0.896×10^{-3} kg m^{-1}s^{-1}) and particle diameter, respectively. The radiation force for simulation is given as follows,

$$\boldsymbol{F}_r(\boldsymbol{r}) = -\frac{dU}{d\boldsymbol{r}} = -\frac{4\boldsymbol{r}}{w^2}U\exp\left(-\frac{2|\boldsymbol{r}|^2}{w^2}\right). \tag{3}$$

Due to the computational time of the simulation, here we simply assume the Gaussian optical potential (U). The width (w) corresponds to half wavelength of the blue- and red-detuned lasers. We confirmed that when the radiation force is zero ($U = 0$), the mean value and mean square displacement satisfy the following equation based on Stokes-Einstein equation,

$$\langle\Delta x\rangle = \langle\Delta y\rangle = \langle\Delta z\rangle = 0, \tag{4}$$

$$\left\langle\Delta x^2\right\rangle = \left\langle\Delta y^2\right\rangle = \left\langle\Delta z^2\right\rangle = \frac{2k_BTh}{\xi}. \tag{5}$$

For the simulation, the initial position of the particle is at the focal spot and we assumed that the initial velocity of the particle is zero. After starting the simulation under the optical potential, we measured the immobilization time when the particle diffuses out and escapes from the focal volume. The shape of the focal volume is assumed to be spherical and its diameter corresponds to wavelength of blue- and red-detuned lasers. We conduct this simulation one thousand times for each condition and simulation results are normalized to one hundred as shown in green line in Fig. 4 below.

4. Theoretical calculation of resonance radiation force based on nonlinear optical response

To compare the experimental results with our previous theoretical proposal [26,27], we calculate the radiation force exerted on dye molecules doped in the particle including the nonlinear optical effects. Here we briefly review the theory and model (for the detail, see our previous papers [26,27]). The time averaged radiation force is a function of electric field ($\boldsymbol{E}$) and the induced polarization ($\boldsymbol{P}$) written as,

$$\langle\boldsymbol{F}(\omega)\rangle = \left(\frac{1}{2}\right)\mathrm{Re}\left\{\int d\boldsymbol{r}\left[\nabla\boldsymbol{E}(\boldsymbol{r},\omega)^*\right]\cdot\boldsymbol{P}(\boldsymbol{r},\omega)\right\}. \tag{6}$$

The electric field of tightly focused laser beam is expressed by using the angular spectrum representation [28]. For the induced polarization, we solve the standard type of density matrix equation using a non-perturbative method. In this calculation, we assumed the dye has three level states including the vibrational state as shown in Fig. 2 (b). From the excitation spectrum of dye-doped particles in Fig. 1(b), we set that the transition energy between 1 and 2 is 2.37 eV and between 1 and 3 is 2.46 eV. The corresponding dipole moments for each transition are set to be 6 and 4 Debye, respectively. The population decay times for the 3-2 state transition, and the 2-1 state transition are assumed to be 3 ps and 4 ns, respectively (the dephasing constants are assumed to be 2 meV). These parameters are chosen from typical Rhodamine molecules. We assumed that 2×10^5 numbers of the dye molecule is contained inside the 500 nm polystyrene particles. Referring the fact that 40 nm dye-doped polystyrene nanoparticles contains 3.5×10^2 dye molecules [17], the 500 nm particles can contain 6.8×10^5 dye molecules (this order is the same with the dye molecule number that we assumed).

Optics EXPRESS

The dye-molecule is located at z = + 300 nm on the z axis where the gradient force becomes large (Fig. 2(a)).

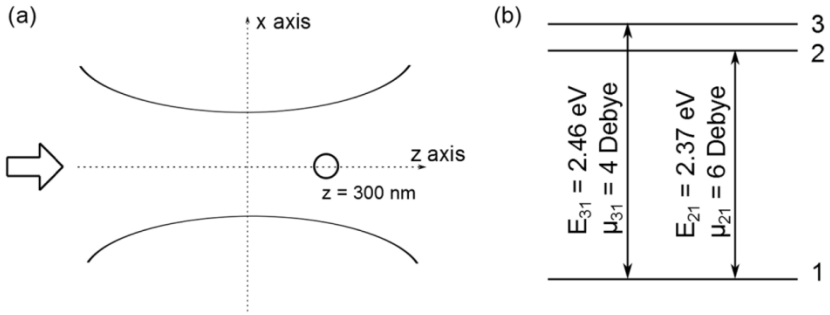

Fig. 2. (a) Sketch of focused laser beam and position of the molecule for the radiation force calculation, and (b) its three level energy diagram with vibrational state.

5. Results and discussion

Figure 3 shows the transmission images measured during the optical trapping of a single bare particle with red-detuned laser. In first five images the color of particle is dark and the particle is located at the bottom side of the focal plane. The particle is pushed by scattering and absorption force to the focus and it is trapped by the gradient force (7th frame). The particle is immobilized at the focus until 18th images and is pushed out along the direction of light propagation. Considering the 33 ms interval of the images, we assume that the immobilization time estimated here has 67 ms uncertainty (the time when the particle is trapped at focus and pushed out from the focus have 33 ms uncertainty). For the event of Fig. 3, the estimated immobilization time is 0.4 s ± 67 ms. We measured the immobilization time one hundred times under the each experimental condition and collected the data into histogram as indicated in Fig. 4. The green dashed-lines in Fig. 4 are the histogram obtained by the simulation with different depth of optical potential. By fitting the green dashed-lines to the experimentally obtained histograms, we estimated the optical potential in the experiment.

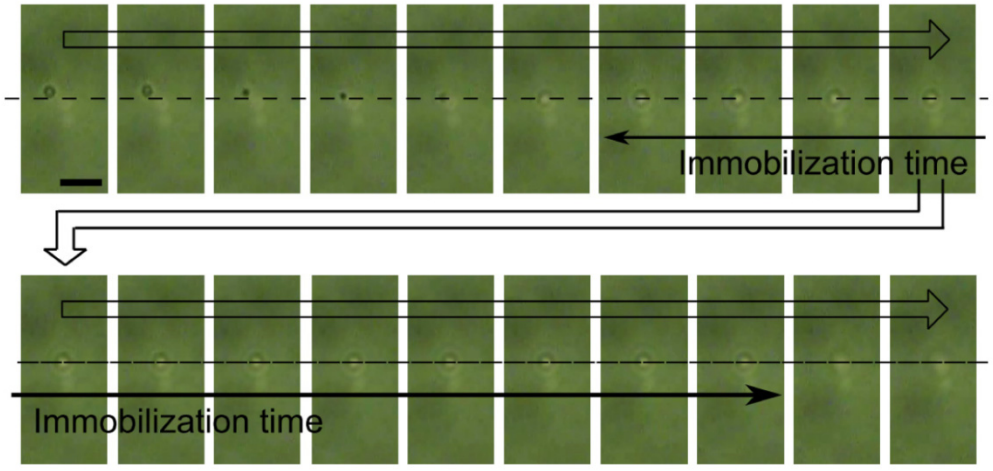

Fig. 3. Typical sequences of transmission images observed during the optical trapping. The sequential images are shown with 33 ms intervals. Horizontal dashed line denotes the vertical position of trapped particles. The red-detuned laser of 8 mW and bare particles are used. The length of black bar is 3 μm.

Here, we compare the histogram of dye-doped particles to that of bare ones at respective laser wavelengths. It is experimentally difficult to change only the wavelength fixing any

Optics EXPRESS

other parameters. For example, beam profile of both lasers, and refractive index and reflection efficiency at both wavelengths are different with each other, leading to an optical artifact in changing wavelength for trapping experiment. The effective irradiation intensity at the focal point under the same laser power is different for blue- and red-detuned lasers. In order to solve the difficulty, we adjusted the laser power to obtain similar histograms for bare particles, on which we examined wavelength dependence of the resonance effect without such optical artifact. Figure 4(a)-(i) and (ii) show the histograms of the immobilization time of bare particles with the red-detuned laser (8 mW) and the blue-detuned laser (10 mW), respectively. Both histograms are quite similar and most of the de-trapping events take place at shorter than 1 s. Indeed, the sum of immobilization time over one hundred events divided by one hundred is both 0.6 s ± 67 ms, which can be defined as effective immobilization time. Therefore, we assumed that the optical potential for bare particle induced by the blue- and red-detuned lasers is almost the same at these laser powers (8 mW and 10 mW, respectively). By comparing the histogram of dye-doped particles with that of bare ones, we are able to discuss the resonance enhancement by dye doping for both lasers.

For the dye-doped particles, they are immobilized longer compared with bare one. As shown in Fig. 4(a)-(iii), the red-detuned laser trapping of dye-doped particles provides the longer immobilization time compared with that of bare one. With increasing the laser power this enhancement appears more clearly in the histogram as shown in Fig. 4(b)-(iii) and 4(c)-(iii), which may be due to the resonance effect. The laser power dependence of the effective immobilization time is summarized in Fig. 5(a) and enhancement is much clear at the higher laser power. With the irradiation of blue-detuned laser, the dye-doped particles are also immobilized at focus longer than bare particles (Figs. 4(a)-(iv), b-(iv) and c-(iv)). Furthermore, we found that the blue-detuned laser trapping gives the deeper optical potential than red-detuned laser trapping for dye-doped particles. This difference between blue- and red-detuned laser trapping becomes more obvious with increasing the laser power. Especially in Fig. 4(c)-(iii-iv) and Fig. 5(b), we confirmed that blue-detuned laser indeed provides the longer immobilization time than that by red-detuned laser. The effective immobilization times in Fig. 4(c)-(iii) and 4(c)-(iv) are 19.5 ± 67 ms and 46.3 s ± 67 ms, respectively. By using the blue-detuned laser instead of red-detuned laser, the effective immobilization time is more than doubled and the number of event which immobilization time is shorter than 10 s becomes about half. The differences in estimated optical potential between blue- and red-detuned lasers are increased with the laser power. In particular, the differences in optical potential are 0.5, 0.6, and 1.25 k_BT for Fig. 4(a), (b) and (c), respectively.

Optics EXPRESS

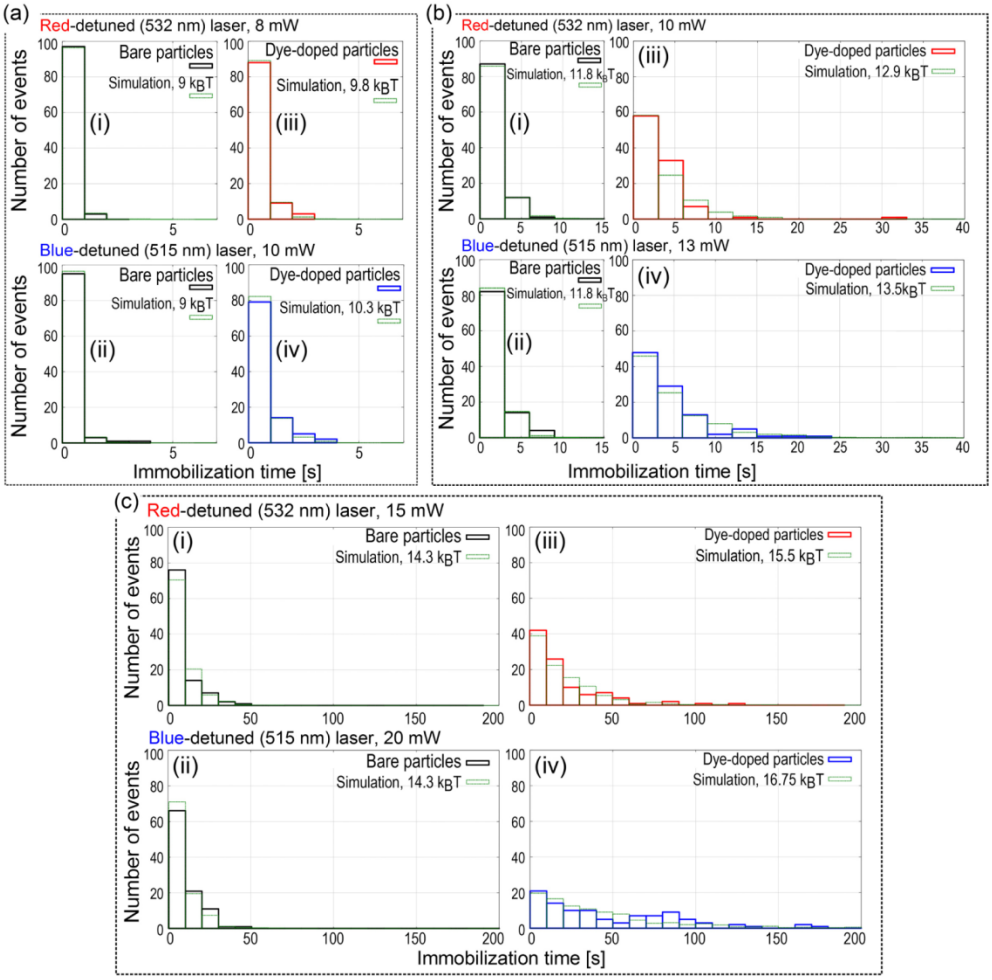

Fig. 4. (a-c) Laser power dependence of histograms of the immobilization time with blue- and red-detuned lasers. (i,ii) Bare particle trapping with red- and blue-detuned lasers, respectively. (iii,iv) Dye-doped particle trapping with red- and blue-detuned lasers, respectively. Green dashed lines are the results from Brownian dynamics simulation under optical potential. The widths of each bar of the histogram are 1, 3, and 10 s, respectively for (a) to (c).

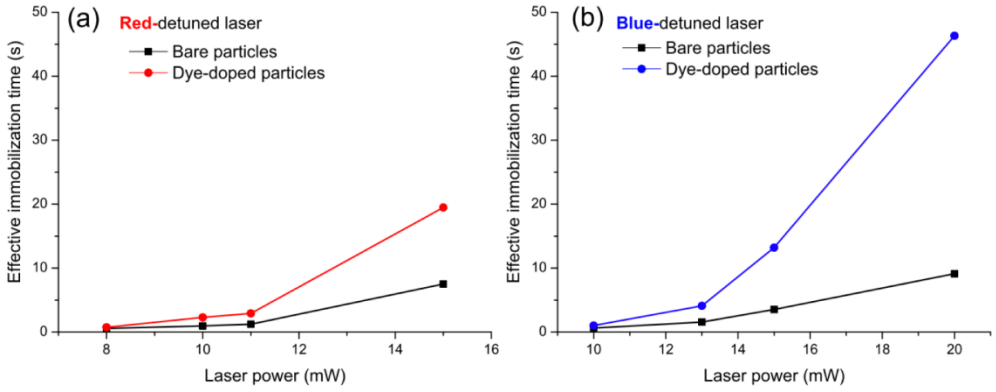

Fig. 5. Laser power dependence of the effective immobilization time with (a) red- and (b) blue-detuned lasers.

Optics EXPRESS

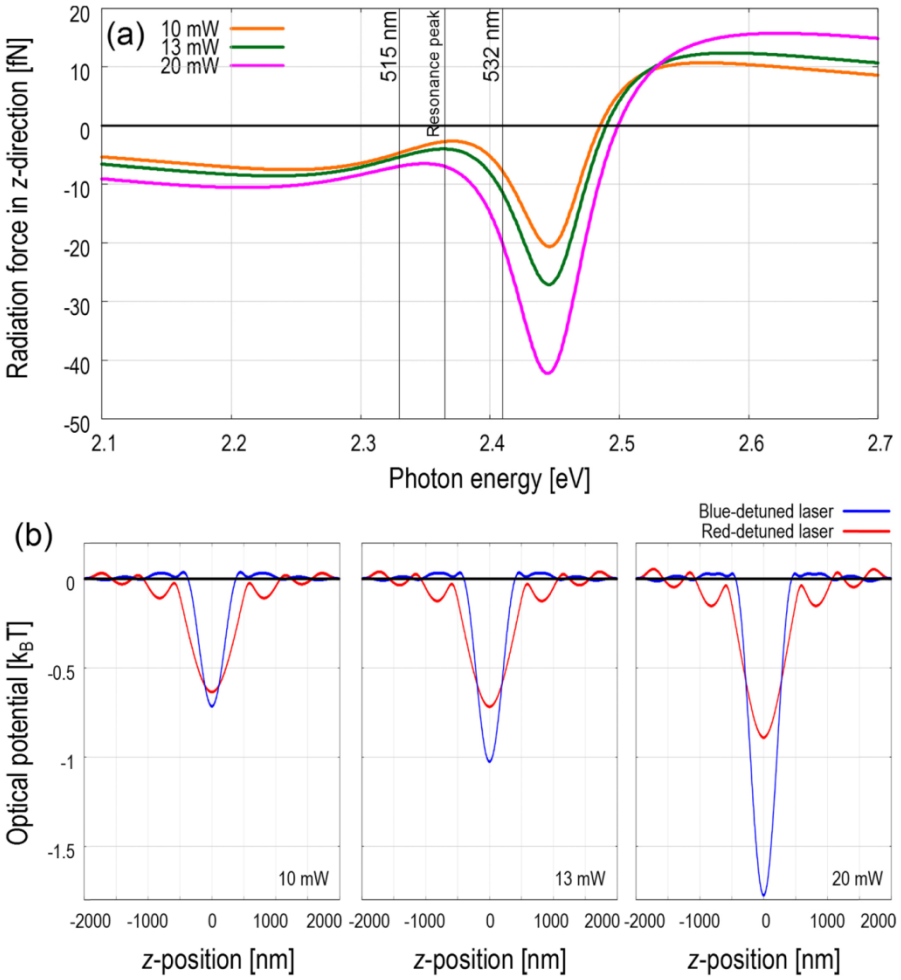

Fig. 6. (a) Photon energy dependence of radiation force exerted on dye molecules along the direction of light propagation (z-axis). The laser powers of orange, green, and pink lines are 10, 13, and 20 mW, respectively. (b) Spatial dependence of optical potential induced by blue- and red-detuned lasers. From the left to right figures, laser power for the calculation is 10, 13, and 20 mW, respectively.

Figure 6(a) shows the photon energy dependence of the radiation force in z-direction with the laser power of 10, 13, and 20 mW. Here we briefly review our previous theoretical proposal [26,27]. The left and right vertical lines in Fig. 6(a) correspond to the photon energy of the red-detuned and the blue-detuned lasers and we can understand that blue-detuned laser provides the stronger gradient force than the red-detuned laser. Blue-detuned laser excites the dye molecule through 1-3 transition and the population of third state quickly decays to second state due to the vibrational relaxation in pico-second order. Because the pumping rate is faster than the decay rate (nano-second order), population of dye molecule is inverted at second state. Previously in our theory, we also showed that the population of dye at the second state is over than one half under the experiment condition [26,27] and resonantly enhanced induced polarization with blue-detuned laser becomes in phase due to the inversion population under the intense focused laser field.

Figure 6(b) shows the optical potential generated by red- and blue-detuned lasers as a function of *z*-position. The optical potential is calculated by integrating the radiation force along the *z*-axis. The difference in optical potential with the blue- and red-detuned lasers is

Optics EXPRESS

increased with laser power due to the nonlinear optical effects. In particular, the differences are 0.1, 0.3 and 1 k_BT for the laser power of 10, 13 and 20 mW, respectively. As we described in experimental part, the difference in immobilization time also increases with laser power. Therefore, the experimental finding is well interpreted by our previous theoretical calculation of the resonance optical trapping with blue-detuned laser.

6. Conclusion

We have experimentally demonstrated the optical trapping of individual dye-doped and bare polystyrene particles with red- and blue-detuned lasers. Through the measurement on the immobilization time, we have reported that dye-doped polystyrene particles are trapped more efficiently than bare ones for both lasers. Further, we have found that the laser blue-detuned from the resonance peak of the dyes provides the deeper optical potential compared to the red-detuned laser. This result well supports our previous nonlinear optical response theory based on three-level model in which the optical potential is deeper with blue-detuned laser compared with red-detuned one due to inversion population of dye molecule. As the future scope of this work, the experimental confirmation of the inversion population is required and this will provide us a clear evidence to prove our theoretical proposal. Now we plan to perform electronic absorption spectroscopy of individual dye-doped particle with tuning the laser wavelength and understand immobilization time and spring constant in term of electronic property of the dyes.

The present study of the resonance optical trapping can be also extended to various nanomaterials. With tuning the laser wavelength, it will be possible to selectively trap the specific molecules, quantum dots and metal nanoparticles. Previously, we have made another theoretical proposal on the resonance optical trapping with simultaneous irradiation of two lasers [27,29]. There it was pointed out that the frequency difference of these two lasers matches to the vibrational energy of the excited state of dye molecule, which is similar to the mechanism of stimulated Raman scattering. The theoretical calculation showed that the optical potential becomes deeper with two lasers of different wavelength compared to one laser of single wavelength. As in resonance and stimulated Raman scattering, optimizing the laser wavelength relative to electronic transition states may also play a significant role in optical trapping. In near future, efficient manipulation of individual molecules, quantum dots, metal nanoparticles, and various nanomaterials will be achieved based on their quantum mechanical properties.

Funding

The present work is partly supported by the MOE-ATU Project (National Chiao Tung University) of the Ministry of Education, Taiwan, to H.M., the Ministry of Science and Technology, Taiwan to H.M. (MOST 105-2811-M-009-022), and Japan Society for the Promotion of Science (JSPS) KAKENHI Grant Number JP16H06504 in Scientific Research on Innovative Areas Nano-Material Optical-Manipulation to H.I.

Acknowledgment

T. K. deeply acknowledges support from JSPS Postdoctoral Fellowships for Research Abroad.